Lawrence Berkeley National Laboratory
Recent Work

Title
Mass Transport in Bedded Salt and Salt Interbeds

Permalink
https://escholarship.org/uc/item/37x0x866

Authors
Hwang, Y.
Pigford, T.H.
Chambre, P.L.
et al.

Publication Date
1989-08-01

Lawrence Berkeley Laboratory
UNIVERSITY OF CALIFORNIA

EARTH SCIENCES DIVISION

Mass Transport in Bedded Salt and Salt Interbeds

Y. Hwang, T.H. Pigford, P.L. Chambré, and W.W.-L. Lee

August 1989

DISCLAIMER

Mass Transport in Bedded Salt and Salt Interbeds

Y. Hwang, T. H. Pigford, P. L. Chambré, and W. W.-L. Lee

Department of Nuclear Engineering
University of California

and

Earth Sciences Division
Lawrence Berkeley Laboratory
University of California
Berkeley, California 94720

August 1989

1. Introduction

Salt is the proposed host rock for geologic repositories of nuclear waste in several nations because it is nearly dry and probably impermeable. Although experiments and experience at potential salt sites indicate that salt may contain brine, the low porosity, creep, and permeability of salt make it still a good choice for geologic isolation. In this paper we summarize several mass-transfer and transport analyses of salt repositories. The mathematical details are given in our technical reports.[1,2,3,4]

2. Bedded Salt: Brine Migration

The existence of salt through geologic time is *prima facie* evidence that it is essentially dry and nearly impermeable. If salt contains brine in grain boundaries[5] brine can flow due to pressure differences within the salt. Brine flow can affect the corrosion rate of nuclear waste containers and the transport of radionuclide from waste packages, thus it is paramount to know the direction and magnitude of brine flow.

Brine exists in natural salt as inclusions in salt crystals and in grain boundaries. Brine inclusions in crystals move to nearby grain boundaries when subjected to a temperature gradient, because of temperature-dependent solubility of salt. Brine in grain boundaries moves under the influence of a pressure gradient.[5,6] When salt is mined to create a waste repository, brine from grain boundaries will migrate into the rooms, tunnels and boreholes because these cavities are at atmospheric pressure. After a heat-emitting waste package is emplaced and backfilled, the heat will impose a temperature gradient in the surrounding salt that will cause inclusions in the nearby salt to migrate to grain boundaries within a few years, adding to the brine that was already present in the grain boundaries.

The lithostatic pressure of the surrounding salt, augmented by the compressive stresses of heating, causes salt to creep against the waste container. Creep of the salt will result in consolidated salt completely enclosing a high-level waste container within a few years after em-placement.

After consolidation of salt around the waste package, neglecting the consumption of brine by container corrosion, brine in grain boundaries near the waste package can only migrate outward into the surrounding salt, under the influence of pressure gradients caused by transient heating of the salt. Hot salt near the waste package expands against the waste package and surrounding salt, creating high compressive stresses near the waste package and resulting in pressure above the lithostatic pressure. Brine pressure further increases because grain-boundary brine expands more than does the salt. The pressure gradient causes brine to flow outward into the cooler salt. Outward flow of brine, decreasing temperature and salt creep relieve the pressure gradient on the fluid, which finally relaxes to near-lithostatic pressure. If the waste containers are failed by corrosion or cracking, this outward brine movement can become a mechanism for radionuclide transport. To determine the extent to which advection by brine in grain boundaries is an important transport mechanism for released radionuclides, it is necessary to estimate the time-dependent migration of brine after salt consolidation.

2.1 Numerical Illustration

We consider a typical waste package containing spent fuel from pressurized water reactors.[7] This package contains 5.5 metric tons of uranium and has an initial thermal flux of 928 watts per square meter of surface area. We approximate the normalized thermal flux using the data in Table I. Table II lists the material properties used in these numerical illustrations.

With the relative power history thus obtained, we assume no convective heat transfer and calculate the temperature field around the waste package as a function of radial distance and time using the Numerical Algorithm Group's (NAG) general-purpose quadrature numerical integrator. Figure 1 shows the temperature profile as a function of distance from the surface of the waste package 1 year,

Table I. Relative Power of a Spent Fuel Waste Package PWR, 10 years out of reactor[7]

Years After Emplacement	Relative Power
0	1.000
5	0.841
10	0.750
15	0.683
20	0.625
30	0.524
50	0.389
70	0.303
100	0.240
300	0.100
500	0.070
800	0.050
1000	0.045

10 years and 100 years after emplacement in salt. For a waste package enclosed by consolidated salt, the time derivative of the relative temperature serves as the input and driving force for brine migration.[1] We compute brine migration velocity in salt as a function of radial distance and time using the Numerical Algorithm Group's (NAG) general-purpose quadrature numerical integrator D01AJF. In Figure 2 we plot the local brine pressure, relative to the far-field brine pressure, as a function of radial distance and time. After creep closes the annular space between the waste package and the emplacement hole wall, the pressure of brine rises above the lithostatic pressure because of thermal expansion of the hotter salt and brine. The built-up pressure relieves rapidly as brine flows outwards into cooler salt. In 100 years there is almost no pressure gradient and brine migration has become negligible. In 100 years the brine pressure in the immediate vicinity of the waste package is slightly less than the far-field brine pressure. At these times, brine will move toward the waste package.

Using the results shown in Figure 2 and the material properties in Table II, the Darcian brine migration velocity can be calculated. The results for 0.1 year, 1 year and 10 years are shown in Figure 3. The brine migration velocities are very low, of the order of micrometers per year. Brine flow is highly transient and is localized to the few meters of salt near the waste package. The maximum velocity occurs a few meters from the waste package and essentially disappears within ten years. Brine migration back towards the waste package occurs, but the reverse migration is weak and occurs at later time a few meters from the waste package.

Table II. Parameter Values Used in Salt Calculations (After McTigue,[6] for the Salado Formation, Delaware Basin, New Mexico)

Property	Value	Units
Conductivity (Λ)	6.60	$W\ m^{-1}K^{-1}$
Heat Capacity	1.89×10^6	$J\ m^{-3}K^{-1}$
Drained Bulk Modulus ($\mathcal{K}$)	20.7	GPa
Fluid Bulk Modulus ($\mathcal{K}_f$)	2.0	GPa
Solid Bulk Moduli ($\mathcal{K}'_s, \mathcal{K}''_s$)	23.5	GPa
Shear Modulus (G)	12.4	GPa
Porosity (ϵ)	0.001	
Permeability (k)	10^{-21}	m^2
Fluid Expansivity (α_f)	3.0×10^{-4}	K^{-1}
Solid Expansivity (α'_s, α''_s)	1.2×10^{-4}	K^{-1}
Fluid Viscosity (μ)	1.0×10^{-3}	Pa· s
$B = \left\{ 1 + \epsilon \frac{\mathcal{K}(1-\mathcal{K}_f/\mathcal{K}''_s)}{\mathcal{K}_f(1-\mathcal{K}/\mathcal{K}'_s)} \right\}^{-1}$	0.93	
Poisson's Ratio (ν)	0.25	
Undrained Poisson's Ratio	0.27	
b'	29.0	$kPa\ K^{-1}$
Fluid Diffusivity (d)	0.16×10^{-6}	$m^2\ s^{-1}$
Thermal Diffusivity (κ)	3.5×10^{-6}	$m^2\ s^{-1}$
$\varphi = \sqrt{d/\kappa}$	0.21	

To investigate the sensitivity of our results to uncertainty in material properties, we varied the permeability from 10^{-20} m^2 to 10^{-22} m^2. The resultant brine migration velocities are shown in Figure 4. Although the permeability is varied a hundredfold, the peak velocity varies only fourfold. The tendency for higher velocities at higher permeability is offset by the more rapid relaxation of the pressure-driving force at higher permeability.

3. Release Rates in Salt by Diffusion

In 1985 Pigford and Chambré proposed[8] a method of predicting radionuclide release rates in a salt repository of high-level nuclear waste, based on mass-transfer analysis. Recognizing that within a few years after the emplacement of heat-emitting waste packages salt creep is likely to close the air gap between a waste container and the

ment of heat-emitting waste packages salt creep is likely to close the air gap between a waste container and the borehole wall, it was proposed that thereafter release rate of dissolved species from the waste solid is likely to be governed by mass transfer into brine in grain boundaries in the surrounding salt and in intersecting interbeds of other rock. Because of the low expected migration velocities of brine in the consolidated salt, mass transfer dominated by diffusion is likely. If so, many of the mass-transfer analyses previously developed could be adapted for predicting release rates in a salt repository.

Subsequent analyses of creep closure and consolidation by Brandshaug[9] show that consolidation is expected within a few years after emplacement.

Because of the extremely small brine migration velocities after emplacement of waste packages predicted in Figure 3, mass transfer of radioactive species dissolved in the brine is likely to be controlled by molecular diffusion.

Here we apply analytic solutions for the rate of diffusive mass transfer of dissolved species through a porous medium to predict radionuclide release rates from waste packages in salt. This analysis shows that for the parameter values selected here, and for containment times of over 300 years, release rates from individual waste packages in salt can meet the U. S. Nuclear Regulatory Commission's (USNRC) performance objective for the engineered barrier system.[10]

The waste container is conservatively assumed to have failed during consolidation or shortly thereafter, so that brine at the waste surface begins to dissolve the spent-fuel waste and its radioactive inventory. The dissolution rate of spent fuel is assumed to be limited by uranium solubility and diffusion into brine contained in the grain boundaries of the surrounding salt. Actinides and other low-solubility constituents are assumed to be released congruently. Iodine, cesium, and and other readily-soluble constituents in fuel-voids and grain boundaries are assumed to dissolve instantaneously in brine that enters failed waste packages. Their release rate into surrounding salt is limited by diffusion.

Low-Solubility Species

Figure 5 shows the release rates of low-solubility species. For the parameter values used, the release rates are well below the USNRC limits. For a UO_2 matrix solubility under oxidizing conditions of 50 g/m^3, the release rates are proportionally higher, but still much below USNRC limits.

Readily Soluble Species

In spent-fuel a fraction of the total inventory of cesium

and iodine accumulates in fuel-cladding gaps, voids, or grain boundaries and is expected to dissolve rapidly when groundwater or brine penetrates the fuel cladding. Even though dissolution may be rapid, the rate of release of these soluble species from the waste package will be limited by their rate of mass transfer into the surrounding porous media. Chambré has developed the analytic solution for the fractional release rate of readily soluble radioactive species, assuming instantaneous dissolution of the soluble species into a volume V of ground water or brine that has penetrated in the waste package voids at $t = 0$, and assuming that the ground-water/brine flow rate is small enough that mass-transfer into surrounding porous rock is controlled by molecular diffusion. We assume that the surrounding porous rock is in direct contact with the well-mixed void liquid (Figure 6).
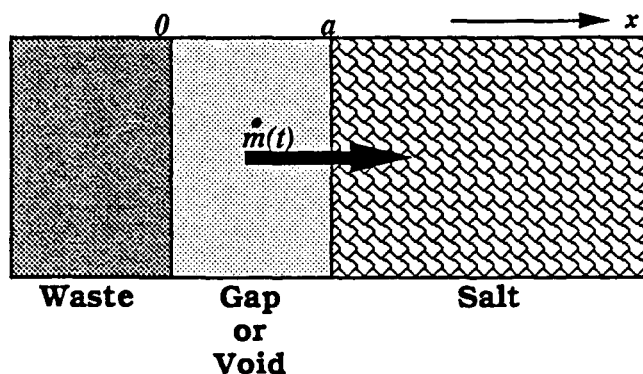

Figure 6. Release of Soluble Species into Salt

For readily soluble species the time-dependent fractional release rates, normalized to initial inventories, from a void of 0.45 m^3 per package, are shown in Figure 7 for a diffusion coefficient of 10^{-7} cm^2/s, for retardation coefficients of 10 and 1 for Cs and I respectively. The release rates for ^{135}Cs and ^{129}I are below the calculated USNRC limits for all times shown. For ^{137}Cs the calculated USNRC limit is exceeded until about 300 years when practically all of the ^{137}Cs has decayed. However, a container that delays releases for 300 years or more would result in negligible release of ^{137}Cs.

4. Interbeds: Mass Transport with Flow

Salt is quite pure in salt domes, but bedded salt is interlaced with layers of sediments that may be capable of conducting water. We need to determine whether interbeds in bedded salt constitute a significant pathway for radionuclide migration.

A waste cylinder of radius r_1 is emplaced in a borehole of radius r_2, intersected by an interbed of thickness $2b$ and porosity ϵ_1, as shown in Figure 8. Consolidated salt,

3

of porosity ϵ_2, is in the annular space between r_1 and r_2. We assume that interbed flow at velocity v is sufficiently large that the Peclet Number Pe= $r^2 v/D$, where D is the diffusion coefficient, exceeds 4. The steady-state mass transfer resistance for potential flow of interbed water around the cylinder is calculated from our mass-transfer equations.[11] The steady-state diffusive mass transfer of a species of solubility c_s to the interbed aperture is calculated from the analysis by Kang et al.[12] through the salt layer. The resulting fractional release of a species with a solubility of 0.001 g/m^3 and the parameters of Table III is shown in Figure 9 as a function of Peclet number.

Table III. Data for Steady-State Interbed Calculations

Radius of waste cylinder	0.31 m
Length of waste cylinder	3.65 m
U-238 inventory	5.4×10^6 g
Crushed salt thickness	3 cm
Crushed salt porosity	0.001
Interbed thickness	1.0 cm
Interbed separation	0.5 m
Interbed porosity	0.01
Diffusion Coefficient	10^{-7} cm^2/s
Uranium solubility	0.001 g/m^3

5. Interbeds: Transient Diffusion from a Waste Cylinder

If the interbed flow is small (Pe$\ll$ 4) diffusion is the only transport important mechanism. Here we adopt [4] analytic solutions[13] for transient diffusion of solubility-limited species from a waste cylinder intersecting a planar fracture. At low flow it is important to calculate transient diffusion into the interbed and into the salt surrounding the waste cylinder. Tables IV and V show parameter values used.

Table IV. Salt Properties Used in Transient Diffusion

Parameter	Units	Salt	Interbed
Diffusion coefficient	cm^2/s	10^{-7}	10^{-7}
Porosity		0.001	0.01^5
Interbed half-width	m		1×10^{-3}

Figure 10 shows the dimensionless flux into the interbed as a function of at various values of the Fourier number t. In Figure 10, at early times such as t=0.1 or about 600 years on the real time scale, the flux into the interbed

of all species is about the same, except for extremely short-lived ones. At larger t, such as t=10 or 100, long-lived species show markedly lower dimensionless fluxes, because for shorter half-life species radioactive decay increases the gradient for diffusion.

Table V. Nuclides Properties

Species	Decay Constant (a^{-1})	Retardation Coefficient in Salt	Retardation Coefficient in Interbed
U-234	2.81×10^{-6}	1	20
Np-237	3.24×10^{-7}	1	20
Pu-239	2.84×10^{-5}	1	20

Figure 11 shows the dimensionless flux into the salt as a function of distance into the salt for different Fourier numbers. At t=0.1, the dimensionless flux in the vicinity of salt/interbed interface is smaller than that further away from the interface. This is due to the diffusion from the interbed to the salt. Because the assumed porosity in the interbed is higher than the porosity in the salt, there is more rapid diffusion of the species in the interbed. The diffusion of the species from the interbed into the salt reduces the gradient for diffusion from the waste cylinder directly into salt, hence the lower flux closer to the salt/interbed interface. As time increases this region influenced by the interbed expands as shown in Figure 11.

Because this analysis was originally developed for transient diffusion from a waste cylinder into a rock fracture with low fracture flow, there is some interest in comparing the overall releases from a waste cylinder facing an interbed in salt and a waste cylinder facing a fracture in granite. In this section, we compare the integrated releases from a waste cylinder of length L. Figure 12 shows the instantaneous mass fluxes, divided by $4\pi r_1 c_s$, into salt and granite using the data in Table VI.

Table VI. Salt and Granite Data used in Comparison

	Porosity	Diffusion Coefficient cm^2/s	Retardation Coefficient	Saturation g/m^3
Salt	0.001	10^{-7}	20	10^{-3}
Interbed	0.01	10^{-7}	1	10^{-3}
Granite	0.01	10^{-5}	500	10^{-3}
Fracture	1	10^{-5}	1	10^{-3}

Although porosities are higher in fracture/interbed, the total mass transfer rate from the waste cylinder is pre-

dominantly from diffusion directly into rock or salt, because of the greater interfacial surface area compared to that of the fracture/interbed aperture. The product of porosity and diffusion coefficient of salt is approximately 10^{-3} times less than that of granite, so the mass transfer rate to the surrounding salt is almost 10^{-3} times less than that of granite.

6. Conclusions

We present an analysis of pressure-driven brine migration in salt. We consider a high-level waste package emplaced in a borehole in salt and backfilled with salt. A few years later salt has consolidated around the waste package. Using our approach and the particular set of parameter values, brine migration after consolidation is of a small magnitude, with Darcy velocities of the order of micrometers per year. Advective transport of dissolved contaminants by brine migration is slow compared to diffusive transport in consolidated salt. Brine migration in consolidated salt is very localized, within a few meters from the waste package, and highly transient, fading to even lower velocities within about ten years.

In a repository containing high-level waste surrounded by consolidated salt, radionuclides dissolved in brine at the waste surface will transport into grain-boundary brine in the surrounding salt by molecular diffusion and by brine migration. For the parameters considered, diffusive transport is more important.

We also calculate mass fluxes from an infinitely long bare waste cylinder in salt, facing an interbed. At the source a constant concentration boundary condition is imposed. If this concentration is the solubility, then this is a conservative analysis. We have also calculated fractional release rates into the interbed. All calculations show releases are low for the parameter values used in the numerical illustrations. The interplay between diffusion from the waste cylinder directly into the salt and through the interbed into the salt has been shown.

We have also compared salt and granite as confining rocks for nuclear waste in the context of this analysis. Because the diffusion coefficient and porosity are lower in salt, the mass fluxes are also lower from a waste cylinder in salt.

These examples show that mass transfer analyses are useful tools in performance assessment of salt repositories.

Acknowledgement

References

1. HWANG, Y., P. L. CHAMBRÉ, T. H. PIGFORD and W. W.-L. LEE, "Pressure-driven Brine Migration in a Salt Repository," *LBL-25768*, Lawrence Berkeley Laboratory (1988).

2. HWANG, Y., W. W.-L. LEE, P. L. CHAMBRÉ and T. H. PIGFORD, "Release Rates in Salt by Diffusion," *LBL-25767*, Lawrence Berkeley Laboratory (1988).

3. HWANG, Y., W. W.-L. LEE, P. L. CHAMBRÉ and T. H. PIGFORD, "Mass Transport in Salt Repositories: Steady-State Transport Through Interbeds," *LBL-26704*, Lawrence Berkeley Laboratory (1989).

4. HWANG, Y., W. W.-L. LEE, P. L. CHAMBRÉ and T. H. PIGFORD, "Mass Transport in Salt Repositories: Transient Diffusion into Interbeds," *LBL-26703*, Lawrence Berkeley Laboratory (1989).

5. BREDEHOEFT, J. D., "Will Salt Repositories Be Dry?" *Eos, 69,* 121 (1988).

6. McTIGUE, D. F., "Thermoelastic Response of Fluid-Saturated, Porous Rock," *J. Geophy. Res., 91, B9,* 9533 (1986).

7. Westinghouse, "Waste Package Reference Conceptual Design for a Repository in Salt," *ONWI-517* (1986).

8. T. H. PIGFORD and P. L. CHAMBRÉ, "Mass Transfer in a Salt Repository," *LBL-19918,* Lawrence Berkeley Laboratory (1985).

9. T. BRANDSHAUG, "Estimate of Consolidation of Crushed Salt Around a Spent Fuel Waste Package," *RSI-315,* RE/SPEC Inc. (1987).

10. U. S. Nuclear Regulatory Commission, Disposal of High-Level Radioactive Wastes in Geologic Repositories, 10 *Code of Federal Regulations* 60.113(a)(1)(ii)(B).

11. P. L. CHAMBRÉ, T. H. PIGFORD, Y. SATO, A. FUJITA, H. LUNG, S. ZAVOSHY, and R. KOBAYASHI, "Analytical Performance Models," *LBL-14842,* Lawrence Berkeley Laboratory (1982).

12. C. H. KANG, P. L. CHAMBRÉ, W. W.-L. LEE and T. H. PIGFORD, "Time-Dependent Nuclide Transport Through Backfill into a Fracture," *Trans. Am. Nuc. Soc., 55,* 134 (1987).

13. J. AHN, P. L. CHAMBRÉ and T. H. PIGFORD, "Transient Diffusion from a Cylindrical Waste Solid into Fractured Porous Rock," *Radioactive Waste Mangement and the Nuclear Fuel Cycle,* in press.
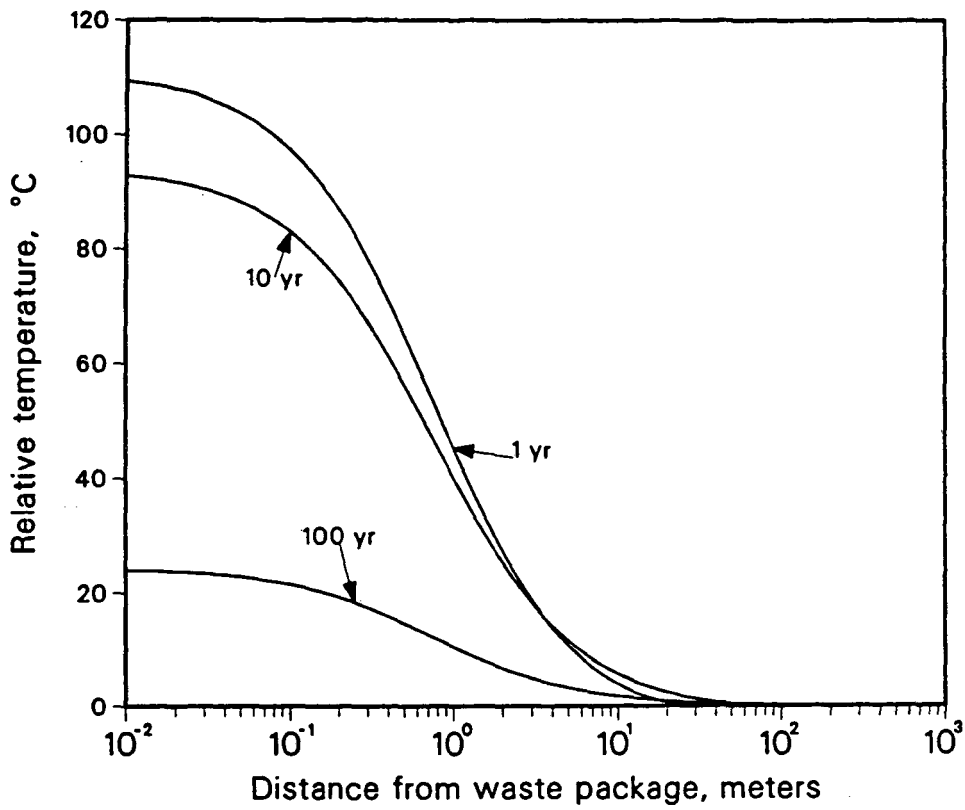
Figure 1. Relative Temperature in Salt after Emplacement
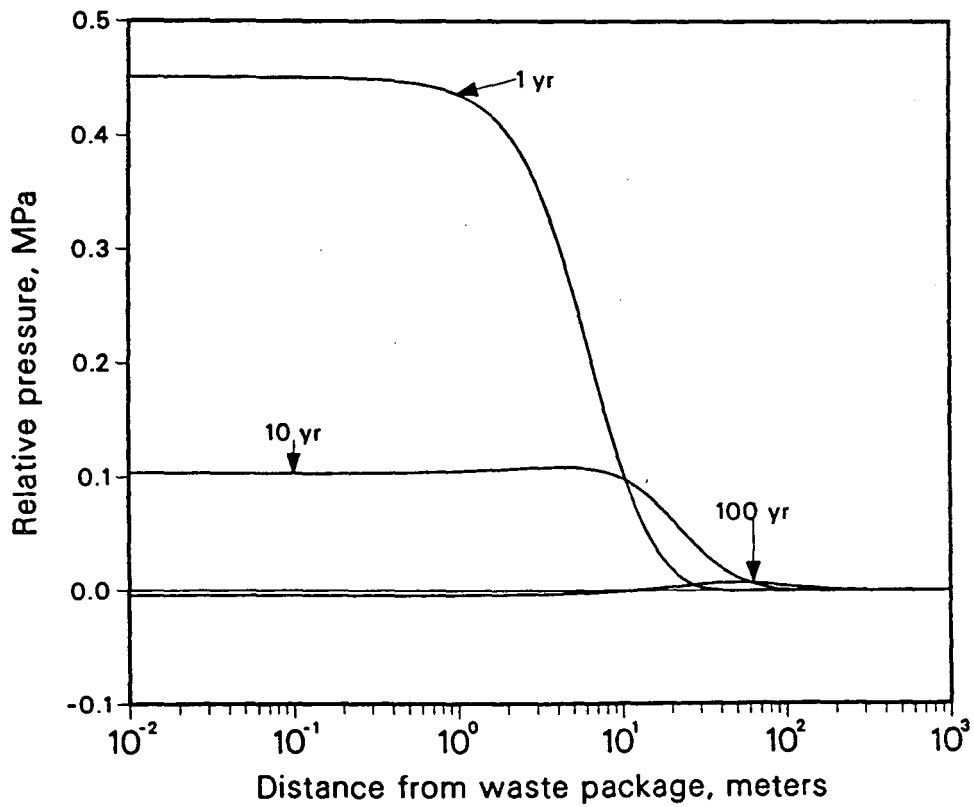

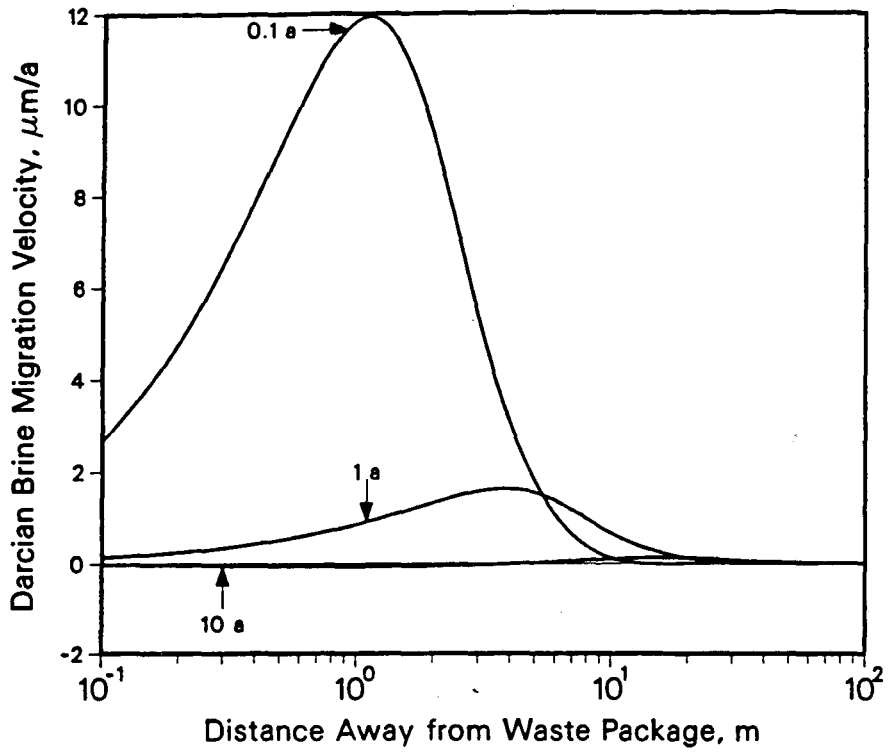**Figure 2. Pressure Profile in Consolidated Salt**

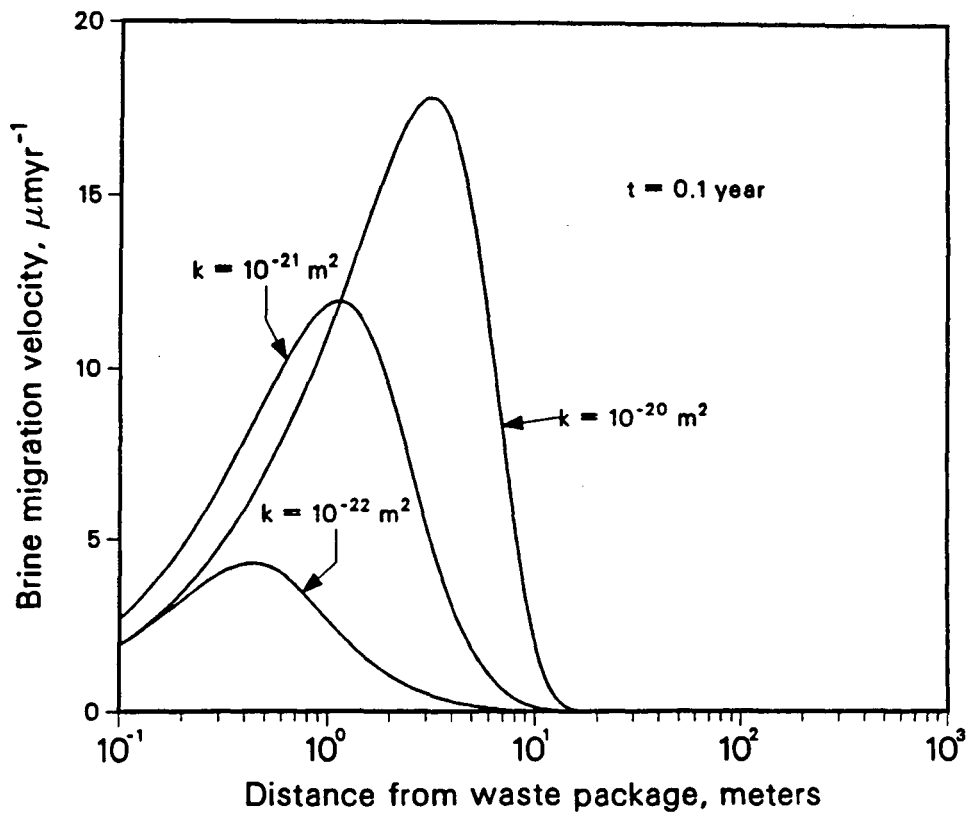Figure 3. Brine Migration Velocities in Consolidated Salt

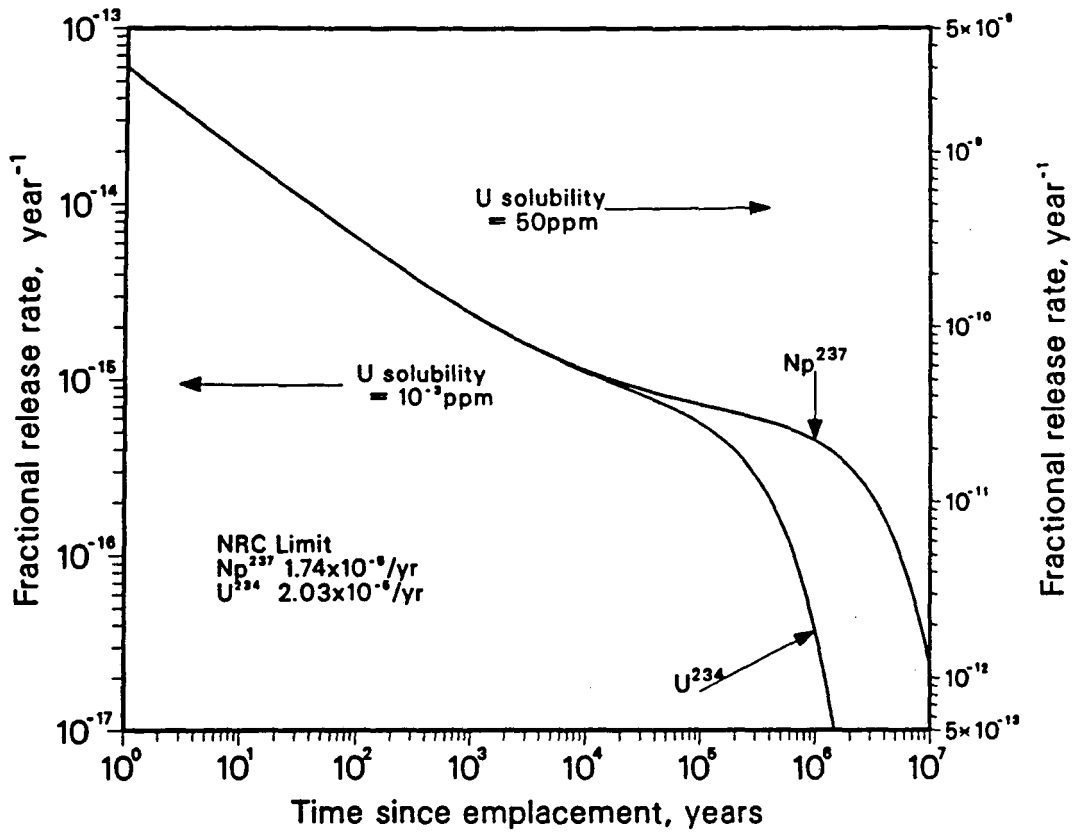Figure 4. Sensitivity of Brine Migration Velocity to Salt Permeability

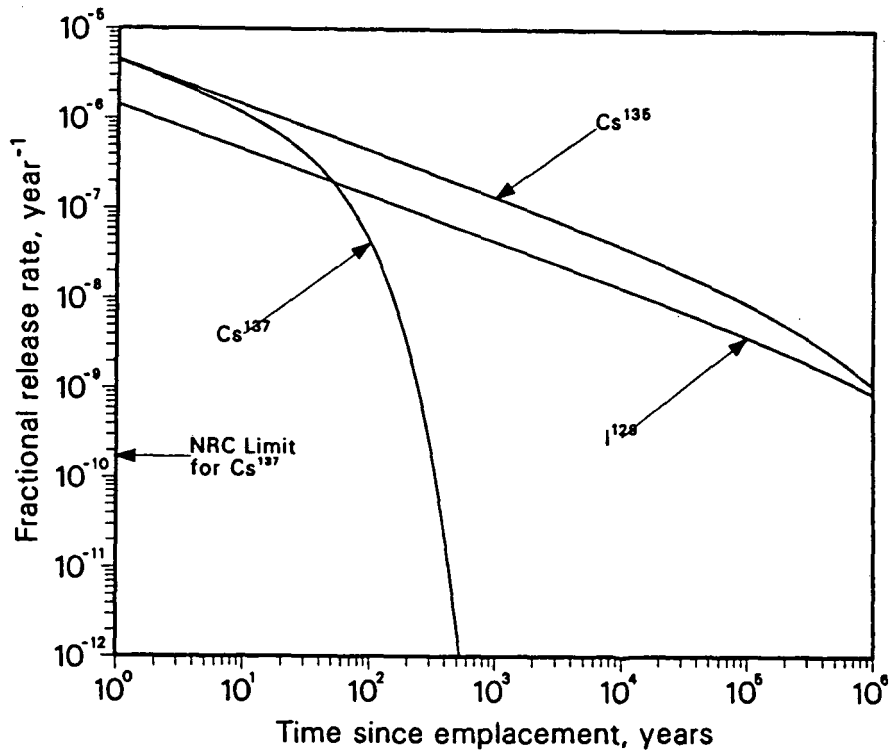**Figure 5. Fractional Release Rates of Low-solubility Species**

In Figure 5, the vertical axes are labeled "Fractional release rate, year^{-1}" (both left and right). The left axis ranges from 10^{-17} to 10^{-13} and the right axis from 5×10^{-13} to 5×10^{-9}. The horizontal axis is "Time since emplacement, years" from 10^{0} to 10^{7}.

Labels on the figure:
- U solubility = 50ppm
- U solubility = 10^{-3}ppm
- Np^{237}
- U^{234}
- NRC Limit
  Np^{237} 1.74x10^{-8}/yr
  U^{234} 2.03x10^{-6}/yr

Figure 7. Fractional Release Rates of Soluble Species

In Figure 7, the vertical axis is labeled "Fractional release rate, year^{-1}" ranging from 10^{-12} to 10^{-5}. The horizontal axis is "Time since emplacement, years" from 10^{0} to 10^{6}.

Labels on the figure:
- Cs^{135}
- Cs^{137}
- I^{129}
- NRC Limit for Cs^{137}
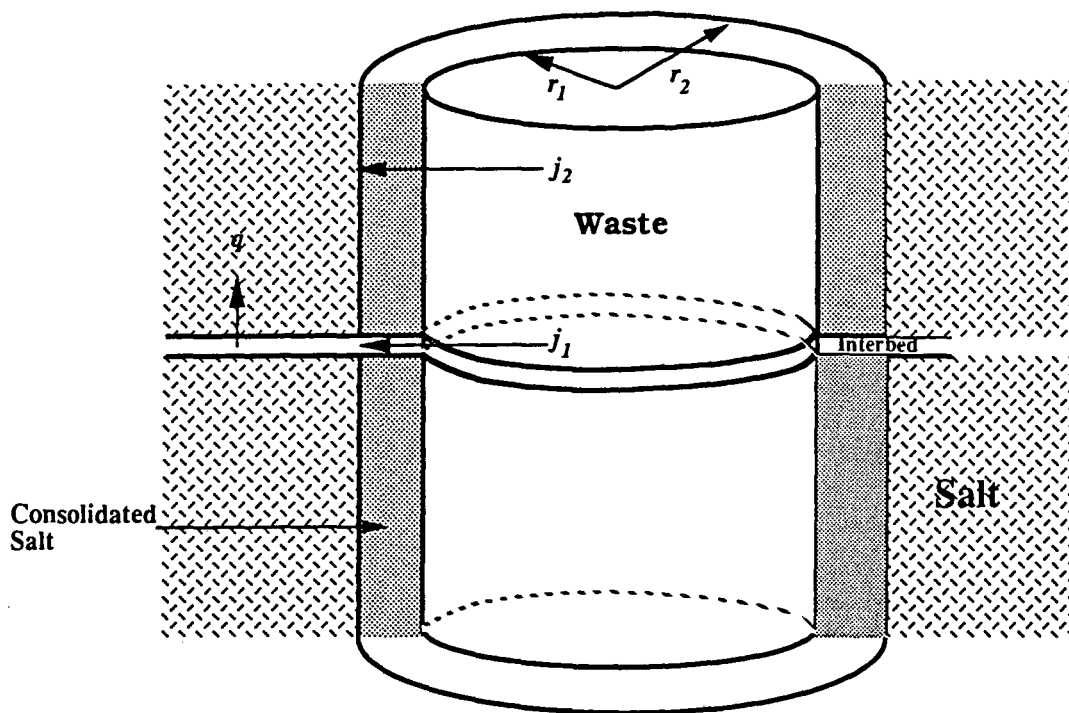
Figure 8. Waste Package Intersected by an Interbed

$D=10^{-7} cm^2/s$
$r_1=0.31$ m
$r_2=0.34$ m
$\varepsilon_1=0.001$
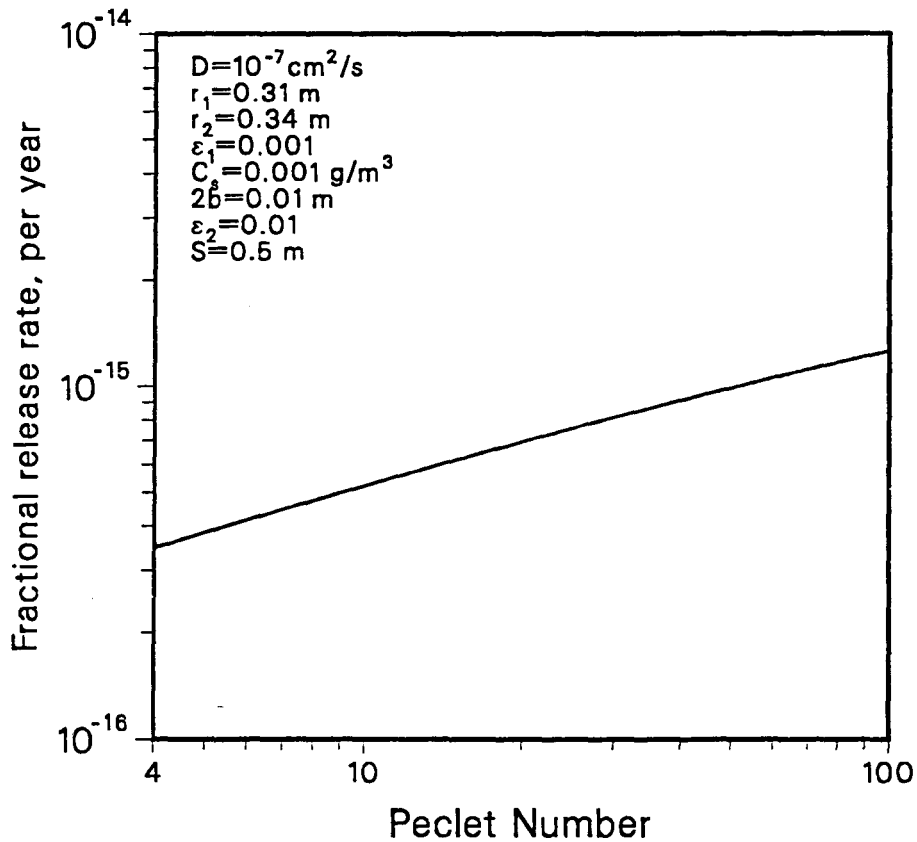$C_s=0.001$ g/m^3
$2b=0.01$ m
$\varepsilon_2=0.01$
$S=0.5$ m

Figure 9. Steady-State Fractional Release Rates of U-238 into an Interbed
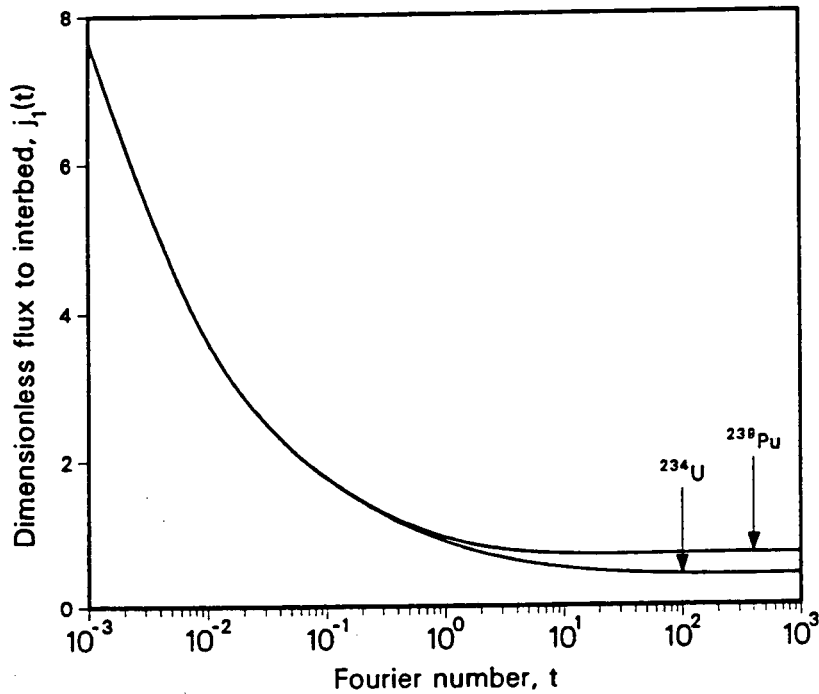
9

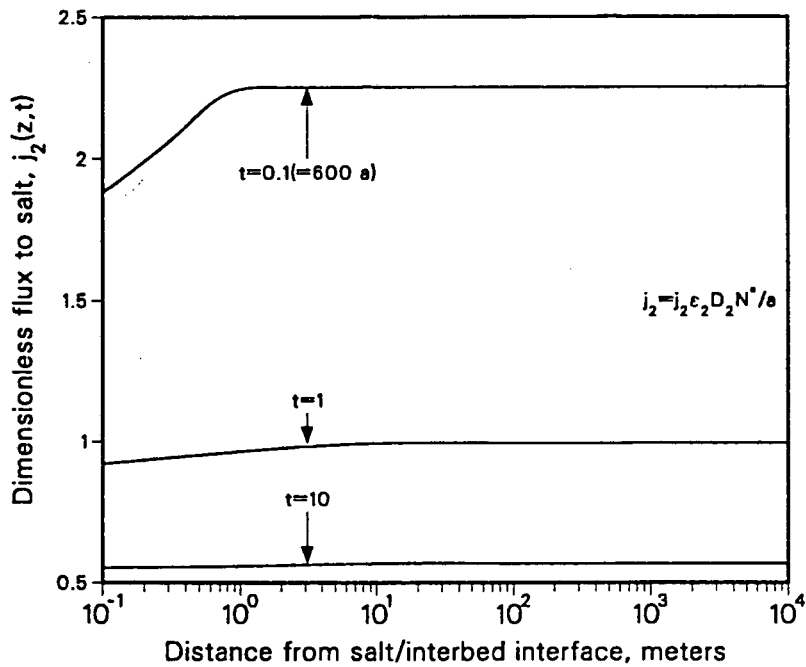**Figure 10. Dimensionless Flux of U-234 and Pu-239 to an Interbed**

Figure 11. Diffusive Flux from the Waste Cylinder Directly into Salt
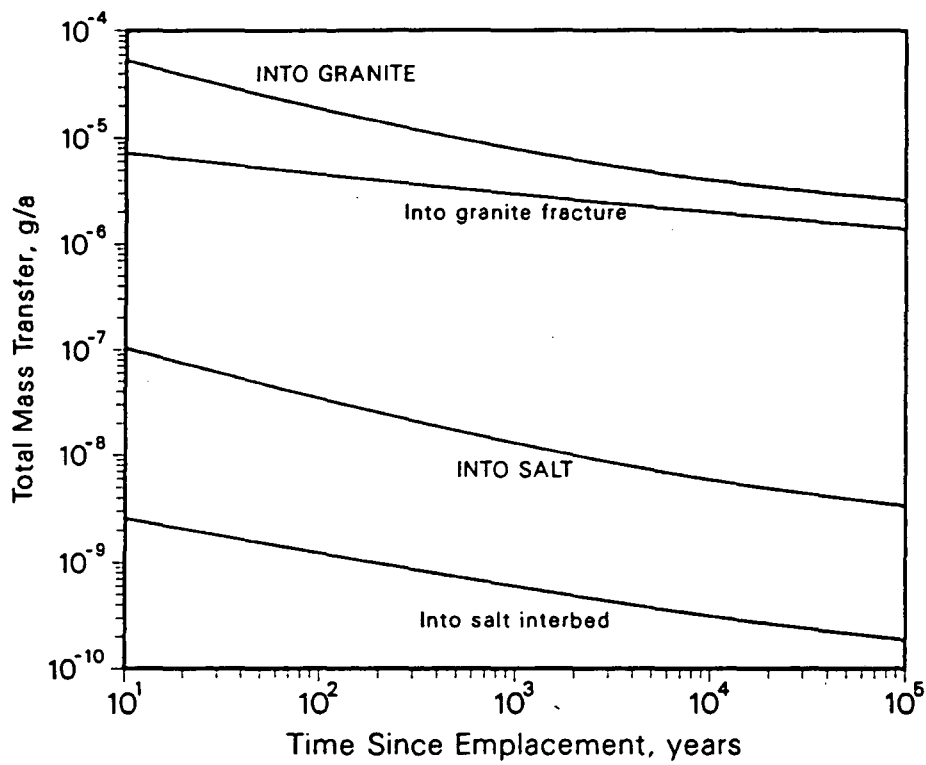
10

Figure 12. Total Mass Transfer of a Stable Nuclide from
a 3.65-m Long Waste Cylinder in Salt and Granite

LAWRENCE BERKELEY LABORATORY
UNIVERSITY OF CALIFORNIA
INFORMATION RESOURCES DEPARTMENT
BERKELEY, CALIFORNIA 94720